# Atmospheric pressure plasma jet utilizing Ar and Ar/$H_2O$ mixtures and its applications to bacteria inactivation*

Cheng Cheng(程 诚)[a)b)†], Shen Jie(沈 洁)[a)], Xiao De-Zhi(肖德志)[a)], Xie Hong-Bing(谢洪兵)[a)], Lan Yan(兰 彦)[a)], Fang Shi-Dong(方世东)[a)], Meng Yue-Dong(孟月东)[a)], and Chu Paul K(朱剑豪)[b)‡]

[a)] *Institute of Plasma Physics, Chinese Academy of Sciences, Hefei* 230031, *China*

[b)] *Department of Physics and Materials Science, City University of Hong Kong, Tat Chee Avenue, Kowloon, Hong Kong, China*

(Received 10 September 2013; revised manuscript received 7 January 2014; published online 15 May 2014)

An atmospheric pressure plasma jet generated with Ar with $H_2O$ vapor is characterized and applied to inactivation of *Bacillus subtilis* spores. The emission spectra obtained from Ar/$H_2O$ plasma shows a higher intensity of OH radicals compared to pure argon at a specified $H_2O$ concentration. The gas temperature is estimated by comparing the simulated spectra of the OH band with experimental spectra. The excitation electron temperature is determined from the Boltzmann's plots and Stark broadening of the hydrogen Balmer $H_\beta$ line is applied to measure the electron density. The gas temperature, excitation electron temperature, and electron density of the plasma jet decrease with the increase of water vapor concentration at a fixed input voltage. The bacteria inactivation rate increases with the increase of OH generation reaching a maximum reduction at 2.6% (v/v) water vapor. Our results also show that the OH radicals generated by the Ar/$H_2O$ plasma jet only makes a limited contribution to spore inactivation and the shape change of the spores before and after plasma irradiation is discussed.

**Keywords:** plasma sources, plasma temperature and density, plasma applications

**PACS:** 52.50.Dg, 94.20.Fg, 52.77.–j **DOI:** 10.1088/1674-1056/23/7/075204

## 1. Introduction

Atmospheric pressure plasma jets or plumes are receiving increasing attention because of potential applications to polymer treatment,[1] etching,[2] film deposition,[3] and biomedical applications.[4] Many atmospheric pressure plasma jets utilizing different types of excitation such as DC (direct current) and microwaves have been developed[5–9] and a dielectric barrier discharge plasma jet operating with sinusoidal signals around 10–100 kHz is the most common nowadays.[1,6,10–14] In this device, the dielectric barrier prevents the formation of high temperature arcs. In plasma jets operating on noble gases such as He or Ar, the formation of active OH species is accomplished by dissociation and excitation of $H_2O$ in the air. The influence of water or peroxide vapor addition on the plasma has been discussed.[15–19] For instance, optical emission spectroscopy allows direct investigation of the OH band and other plasma characteristics. Wang *et al.* determined the absolute OH density by adding water vapor to the carrier gas in a continuous atmospheric microwave plasma jet by UV-cavity ring-down spectroscopy (CRDS).[20–22]

The physical characteristics and biological applications of atmospheric pressure plasma jets operating on different gases have been studied[23–31] and the biological effects mainly stem from UV light emission, a high concentration of charged particles, and OH and O radicals generated in the discharge.[32–36] Walsh *et al.* reported that in the linear-field jet, electron transportation was driven downstream to allow more active plasma chemistry.[2] Although there have been many investigations on the inactivation mechanism of atmospheric pressure plasma jets,[6–8,23–36] the contribution of various species in the plasma and their individual efficacy in killing bacteria are still not well understood. OH radicals have been reported to play an important role in sterilization.[6,14,19,32] In these reports they only prove the existence of OH by optical emission spectroscopy, but there is no discussion about the influence of OH concentration on inactivation effects. In this study, a plasma jet with a single electrode is optimized to produce a large amount of OH radicals in the afterglow of the plasma jet by mixing Ar with water vapor. Our objective is to investigate directly the role played by OH radicals in *Bacillus subtilis* spore inactivation and optical emission spectroscopy (OES) is employed to identify the excited species and determine the important plasma parameters such as the gas temperature, electron excited temperature, and electron density in the Ar and Ar/$H_2O$ plasma jets.

## 2. Experimental details

A schematic of the atmospheric pressure plasma jet is depicted in Fig. 1. A copper rod (2 mm in diameter and 100 mm long) was embedded in a quartz tube (2 mm in inner diameter,

*Project supported by the National Natural Science Foundation of China (Grant No. 11005126), the Hefei Institute of Physical Science, Chinese Academy of Sciences Dean Fund, China (Grant No. YZJJ201331), and the City University of Hong Kong Applied Research Grant, China (Grant Nos. 9667066 and 9667069).

†Corresponding author. E-mail: chengcheng@ipp.ac.cn

‡Corresponding author. E-mail: paul.chu@cityu.edu.hk

 

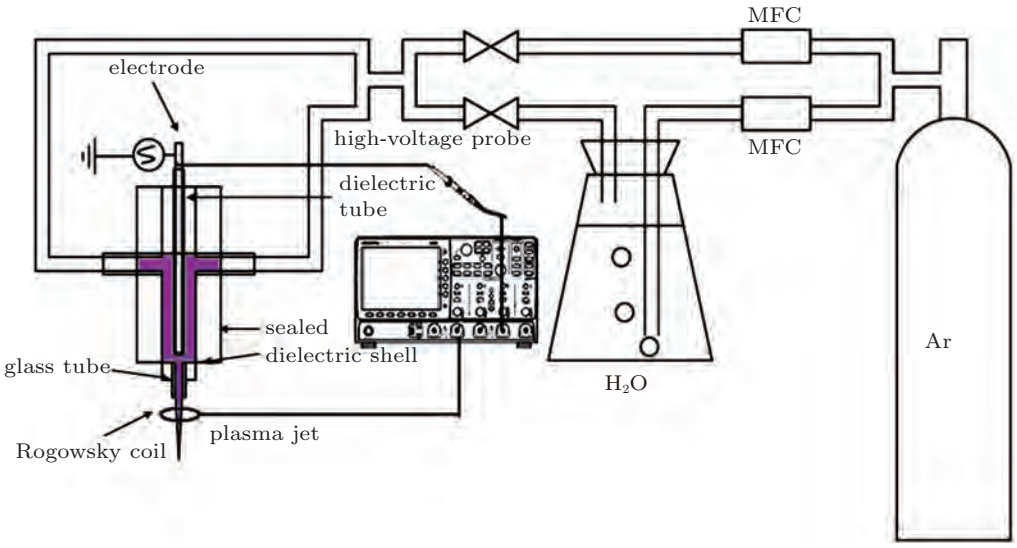


**Fig. 1.** (color online) Schematic diagram of the atmospheric pressure plasma jet.

4 mm in outer diameter, and 80 mm long) with one side sealed as the single electrode and wrapped tightly with a teflon shell . The teflon shell is a hollow cylinder, and its inside diameter and outside diameter are 10 mm and 20 mm respectively. A quartz tube (20 mm in length, 4 mm in inner diameter, and 6 mm in outer diameter) was connected to the shell as a nozzle. An AC power supply with frequencies from 10 kHz to 42 kHz and variable output voltages from 0 kV to 50 kV (peak to peak) was used. Argon (99.99% pure) as the carrier gas was regulated by a gas flow meter and bled directly through the tube and also into water to form a gas mixture of Ar and $H_2O$ vapor at 20 °C. Here, $Ar_{water}$ was the volume of Ar passing through the water and the total gas flow was fixed at 750 $h^{-1}$. The volume ratio of water vapor injection into the plasma jet was $Ar_{water}/Ar_{total}$. The voltages and currents were monitored by a high-voltage probe (P6015A) and a Rogowsky coil via a digital oscilloscope (Tektronix MSO 5104). In order to investigate the electrical characteristics of the plasma jet, a Rogowsky coil was mounted 1 cm away from the nozzle to measure the current. The optical emission from the plasmas was monitored on the AvaSpec-2048-8-RM spectrometer with a grating of 2400 grooves/mm and an optical fiber was located at a distance of 1 cm away from the nozzle of the plasma jet.

The decontamination capability of the atmospheric pressure Ar or Ar/$H_2O$ plasma jet was assessed using *Bacillus subtilis* spores having strong vitality. *Bacillus subtilis* is a gram-positive bacterium with a thicker cell wall than gram-negative microorganisms and a spore-forming vegetative cell produces a highly tolerant spore protected by a multilayer comprising the cortex and protein envelopes. The spore acquires higher resistance to bactericidal actions of various chemical and physical factors. In our experiments, 0.05 ml of the spore suspension ($1.16 \times 10^8$ spores/ml) was deposited on a polytetrafluoroethylene (PTFE) sheet (6 mm diameter) and allowed to dry for 12 h in air. The dried samples were exposed to the plasma jet at a distance of 1 cm from the nozzle at a fixed voltage (22 kV) and different water vapor concentrations at a flow rate at 750 $h^{-1}$. After the plasma treatment, each sample was put in 5 ml of sterilized distilled water and the spores were removed from the PTEF sheet using a vortex stirrer and an ultrasonic generator. One-tenth of a milliliter of each sample was spread onto an Agar plate and after incubation at 37 °C for 24 h, the colonies were counted. In order to reduce errors in plasma inactivation, three independent experiments were performed under the same conditions, and the colony counting result was the average of the three independent experiments.

## 3. Results and discussion

A high voltage of 22 kV at a frequency of 38 kHz is sufficient to sustain a cold plasma jet with up to 7.8% $H_2O$ vapor as shown by the photos of the plasma jet with 0%–7.8% $H_2O$ vapor concentrations in Fig. 2. The plasma jet is more than 30 mm long without $H_2O$ vapor and shortens to about 20 mm as the $H_2O$ vapor concentration reaches 5%. When the $H_2O$ vapor concentration is above 7.8%, the plasma is only sustained inside the quartz tube and becomes weaker.

Optical emission spectroscopy is a common technique to determine the various plasma parameters such as the excited species, gas temperature, excitation temperature, and electron density. Photon counting is carried out for 80 ms and repeated 100 times for data accumulation. Figure 3 shows the optical emission intensity of the Ar and Ar/$H_2O$ plasma jets in the range of 200–1050 nm. The intensity of OH (309 nm) reaches the highest value at a water concentration of 2.6% and then decreases significantly as the water concentration is increased further. In this study, we specifically focus on the OH concentration because it is considered as an important factor for inactivation. Excited oxygen atoms (emission lines at

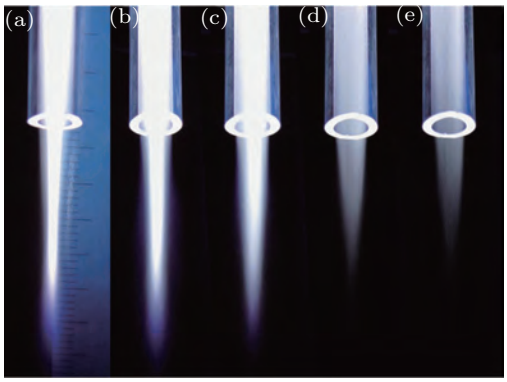


**Fig. 2.** (color online) Photographs of the atmospheric pressure plasma jet with different volume ratios of $H_2O$ vapor: (a) 0%, (b) 1.3%, (c) 2.6%, (d) 5.2%, and (e) 7.8%.

777.2 nm and 844.6 nm) are produced inevitably when the pure Ar plasma jet is operated in open air, and so the effects of the excited oxygen atoms on inactivation must be considered. As reported previously,[7,8,36] the inactivation efficacy increases significantly when a small amount of oxygen is injected into the plasma jet, and it is attributed to the sharp increase in the amount of excited oxygen atoms. However, in our experiments, the intensity of these two lines does not increase significantly as the water concentration is increased, as shown in Fig. 3. Therefore, the effects of the change of the excited oxygen atoms can be neglected and the relationship between the excited oxygen atoms and inactivation is investigated here.

The gas temperature is an important parameter in plasma processing and in an atmospheric pressure discharge,[15,22,37] the rotational temperature $T_r$ of OH ($A^2\Sigma^+$, $v = 0$) can be used to estimate the gas temperature $T_g$. The gas temperature is determined by $T_r$ of OH using the LIFBASE software as shown in Fig. 4[15] and the rotational temperature is about 313 K in the Ar and Ar/$H_2O$ plasma jet. In Bruggeman's report,[38] the rotational temperature based on the OH lines in the liquid containing plasma is unreliable. In order to monitor the slight change in the gas temperature accurately, a thermometer is used, and it is located at a distance of 1 cm away from the nozzle of the plasma jet. The gas temperature in the Ar plasma jet is close to 40 °C (313 K) and decreases to 33 °C (306 K) at 7.8% water vapor, as shown in Fig. 5. At a flow rate of 750 $h^{-1}$, the voltage and current waveforms for different water contents are acquired and presented in Fig. 6. There are two peaks in the current waveform in the discharge in pure Ar during the half-period of the applied voltage. The first peak has a time duration of 1.2 μs and the second one is about 3.3 μs. The maximum current increases to about 200 mA and the current pulse length decreases to 0.9 μs after the addition of water vapor (7.8% (v/v) concentration) to the feed gas. Furthermore, addition of water vapor to the feed gas reduces the current peak duration and increases the maximum current, and the current waveform at a water vapor concentration of 7.8% (v/v) is not symmetrical. Although the maximum current goes up with increasing water concentration, the average discharge power decreases because the current peak duration decreases significantly according to the following expression: $P_{ave} = (1/T)\int_0^t U(t)I(t)\,dt$. The relationship between the gas temperature at different water concentrations and average power is illustrated in Fig. 6. The gas temperature decreases when water vapor is introduced because the average discharge power is reduced.[15]

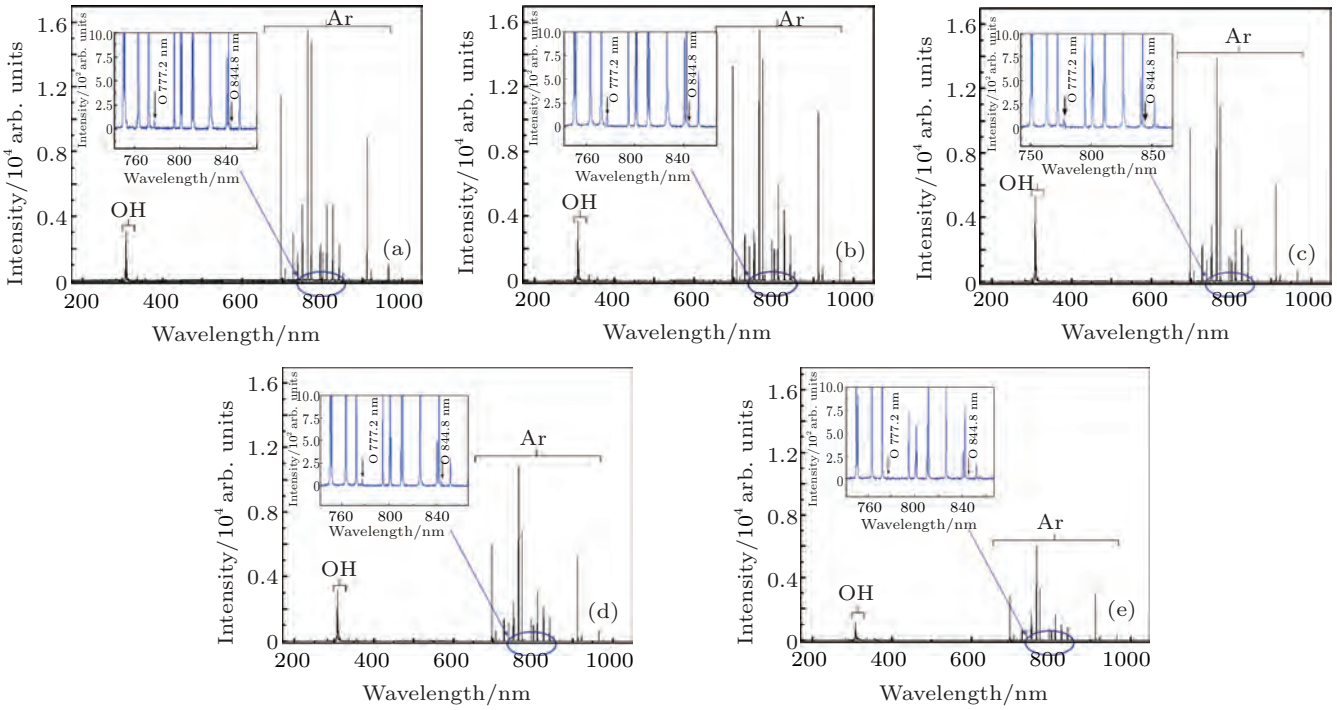


**Fig. 3.** (color online) Axial emission spectra of the plasma jet in the mixtures with (a) 0%, (b) 1.3%, (c) 2.6%, (d) 5.2%, and (e) 7.8% (v/v) $H_2O$ vapor. The input voltage is fixed on 22 kV.

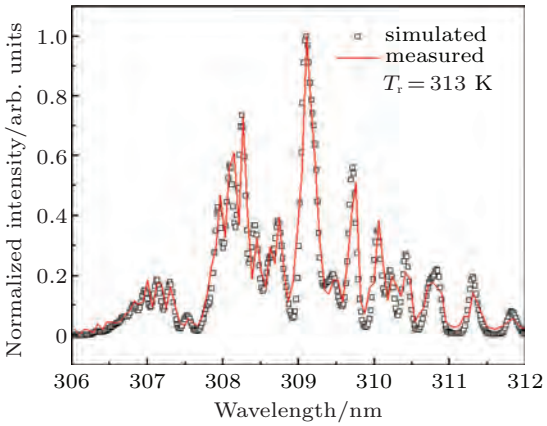


**Fig. 4.** (color online) Fittings of the experimental and simulated spectra of OH radicals with the emission recorded at 10 mm from the edge of the quartz tube (pure Ar).

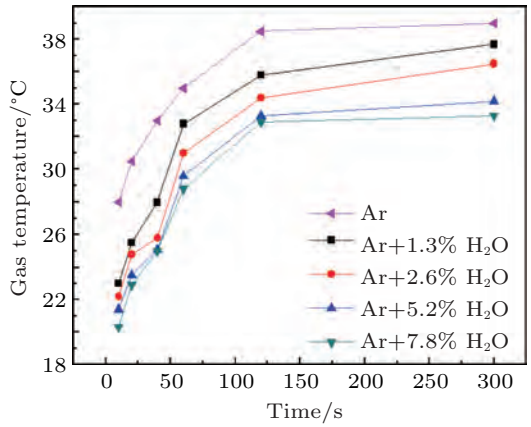


**Fig. 5.** (color online) Gas temperature at different $H_2O$ vapor concentrations measured by a thermometer.

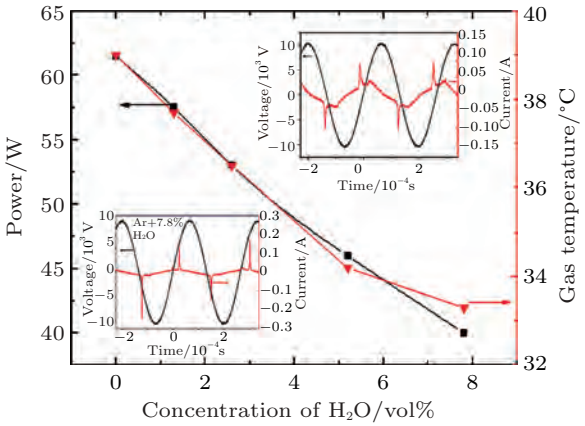


**Fig. 6.** (color online) Relationship of input power versus gas temperature of the plasma jet at different $H_2O$ vapor concentrations.

The excitation temperature $T_{exc}$ of the plasma jet is calculated by the Boltzmann method[39] applied to several excited Ar emission lines and these emission lines are shown in Table 1. By adopting a linear fit, the excitation temperature is found to be 9054 K (0.78 eV) in the Ar plasma jet (Fig. 7). The excitation temperature decreases gradually with water vapor injection increasing and it is 7816 K (0.67 eV) for 7.8% water vapor content. The drop is probably due to collisions between $H_2O$ with excited argon species.[15] As the excitation temperature may be used to estimate the electron temperature,[2] the results suggest that the Ar plasma jet has larger average electron energy.

**Table 1.** Line parameters of the Ar lines.

| $\lambda$/nm | $E_{ki}$/eV | $A_{ki}$/s$^{-1}$ | $g_i$–$g_k$ |
|---|---|---|---|
| 426.65 | 19.549 | $1.64 \times 10^7$ | 6–6 |
| 427.2 | 14.52491 | $7.97 \times 10^5$ | 3–3 |
| 430.01 | 14.50607 | $3.77 \times 10^5$ | 3–5 |
| 433.36 | 14.68829 | $5.68 \times 10^5$ | 3–5 |
| 440.098 | 19.2229 | $3.04 \times 10^7$ | 8–6 |
| 667.73 | 13.47989 | $2.36 \times 10^5$ | 3–1 |
| 435.22 | 19.30534 | $2.12 \times 10^7$ | 2–2 |
| 714.7 | 13.28264 | $6.25 \times 10^5$ | 5–3 |

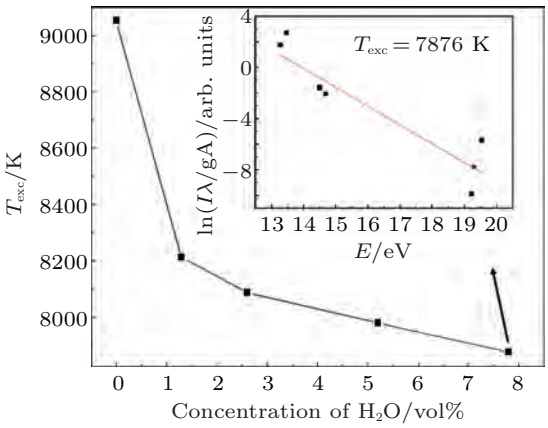


**Fig. 7.** (color online) Electron excitation temperature of the plasma jet at different $H_2O$ vapor concentrations.

The electron density ($N_e$) is determined from the Stark broadening of the $H_\beta$ Balmer series line (486.13 nm) of atomic hydrogen. Hydrogen is present in the discharge as an impurity in the carrier gas (Ar and Ar/$H_2O$). Stark broadening of the $H_\beta$ line is one of the common tools to diagnose the plasma electron density because it depends on the electron temperature.[11,37,40–45] Under the conditions of ~1 atmospheric pressure and $T_g$ of 300 K to 330 K, the most important mechanisms are van der Waals broadening, due to collisions between excited hydrogen and argon atoms, and Stark broadening arising from the interaction between charged particles and excited hydrogen atoms. Both exhibit a Lorentzian profile. In addition, Doppler broadening stemming from the thermal motion of excited hydrogen atoms and instrumental broadening with a Gaussian profile should be considered. Other less important effects such as natural broadening or resonant broadening can be neglected in the high density plasma.

The profiles derived from these mechanisms can be approximated to have the Gaussian or Lorentzian forms and the combined contribution (convolution) is the Voigt profile. The

part of line broadening corresponding only to Stark broadening can be obtained by separating (deconvoluting) Stark broadening from the total broadened profile. Calibration of the instrumental functions is made with a mercury lamp on the Hg I 471 nm line and it is found to be a Gaussian with a full-width at half-maximum (FWHM) of 1.4 Å. Doppler broadening is determined from the gas temperature $T_g$, by the FWHM expression[44]

$$\Delta\lambda_D\ (\text{nm}) = 7.16 \times 10^{-7} \lambda_0 (T_g/M)^{1/2},$$

where $T_g$ is in Kelvin, $M$ is for H expressed in atomic mass units, and $\lambda_0$ is the wavelength of the line in nanometers with a value of 0.005 nm. For the two Gaussian profiles, the convolution is also a Gaussian profile with a total FWHM given by $\Delta\lambda^2_{\text{Gauss}} = \Delta\lambda_1^2 + \Delta\lambda_2^2$.[44]

Convolution of the two Lorentzian profiles also yields a Lorentzian profile with the FWHM given by $\Delta\lambda_{\text{Lorentz}} = \Delta\lambda_1 + \Delta\lambda_2$.[44] The FWHM of van der Waals broadening can be expressed by the following formula:

$$\Delta\lambda_{\text{Waals}} = K_i (T_g/\mu)^{0.3} N,$$

where $\mu$ is the reduced mass of the H–Ar pairs, $N$ is the neutral density which can be derived from the gas temperature $T_g$ using the ideal gas law, and $K_i$ is a constant depending on the spectral line and emitter polarizability with a value of 0.055 nm.[45] The FWHM of Stark broadening is related to the electron density as follows:[11,37]

$$\Delta\lambda_{\text{Stark}}\ (\text{nm}) = 2 \times 10^{-11} (n_e)^{2/3},$$

where the electron density is in $\text{cm}^{-3}$. Each broadening mechanism is independent of each other and the combined line profile is the convoluted line profiles of each mechanism. By comparing the Voigt profile and measured line, the FWHM of Stark broadening $\Delta\lambda_{\text{Stark}}$ is 0.107 nm resulting in an electron density of $3.9 \times 10^{14}$ $\text{cm}^{-3}$ (Fig. 8). The electron densities at a fixed voltage but different water concentrations are shown in Fig. 8, further indicating that the electron density decreases almost linearly with water concentration.

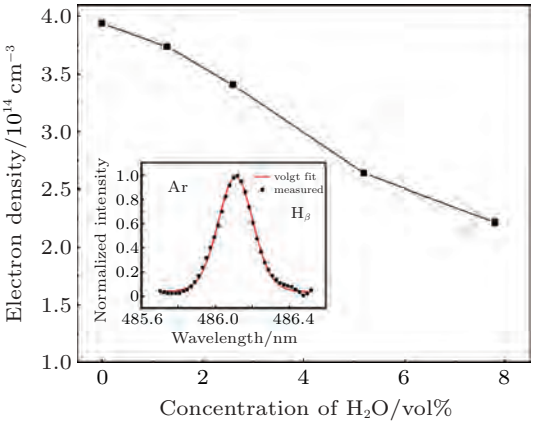


**Fig. 8.** (color online) Electron densities of the plasma jet at different $H_2O$ vapor concentrations.

Figure 9 shows the survival curves of *Bacillus subtilis* spores after exposure to the Ar plasma jet, Ar/$H_2O$ plasma jet, and other entities (UV radiation, heat) generated by the plasma. Because the gas temperature of the plasma jet is only 40 °C, the hot gas flow at 40 °C is used to simulate the plasma gas temperature for inactivation at flow rate of 750 $\text{h}^{-1}$ and it results in no reduction. To study the effects of UV photos generated by the plasma jet, a UV-passing glass is placed above the spore sample and the number of living spores is reduced by one tenth after 5 min of UV exposure. The optimal UV germicidal action occurs between 240–280 nm, but there are no emission lines in this range (Fig. 3) from either the Ar or Ar/$H_2O$ plasma jet. This is the reason why reduction is small after exposure to UV. The results thus illustrate that heat and UV are minor contributors in plasma inactivation. To evaluate whether OH may play the major role, the *Bacillus subtilis* spores are exposed to the plasma jet with 2.6%(v/v) water and the largest emission intensity of OH (309 nm) is observed. The resulting inactivation of spores by the Ar and Ar/$H_2O$ plasma jets are shown in Fig. 9. A 5-min exposure to the Ar atmospheric pressure plasma jet produces nearly 2-log reduction in the number of living *Bacillus subtilis* spores and compared to the Ar plasma jet, the Ar/$H_2O$ plasma jet results in a 0.4-log reduction.

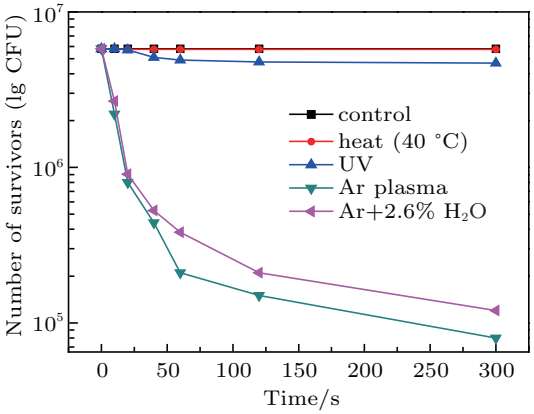


**Fig. 9.** (color online) Survival curves of *Bacillus subtilis* spores treated by the Ar plasma jet at different $H_2O$ vapor concentrations using different plasma parameters (UV, temperature).

In order to verify that O is not the main inactivation factor but rather OH plays the dominant role when water vapor is injected into the plasma jet, figure 10 shows the killed *Bacillus subtilis* spores as well as actinometric measurements using O (777.2 nm and 844.6 nm) in the Ar/$H_2O$ plasma jet when the $H_2O$ concentration is increased from 0 to 7.8%. Compared with our previous results on the Ar/$O_2$ plasma jet,[36] the intense excited oxygen atom emission lines from the Ar/$H_2O$ plasma jet change only slightly as the water concentration is

increased. In addition, it is obvious that the optimal inactivation efficacy does not correlate with the maximum O emission intensity but instead the maximum OH emission intensity (Fig. 11). Hence, the main reason for the change of inactivation efficacy is the change in OH as water vapor is introduced to plasma jet.

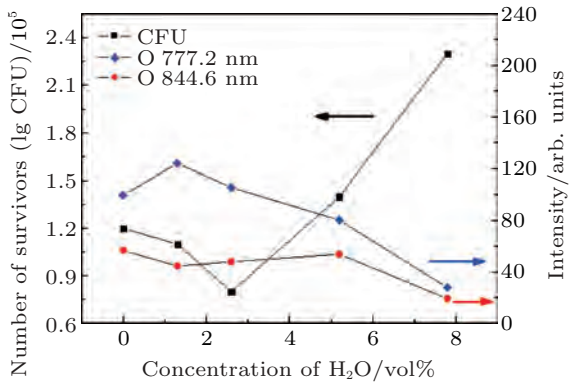


**Fig. 10.** (color online) Survival curves of *Bacillus subtilis* spores and O (777.2 nm and 844.6 nm) intensity as a function of $H_2O$ vapor concentrations (treatment time = 5 min).

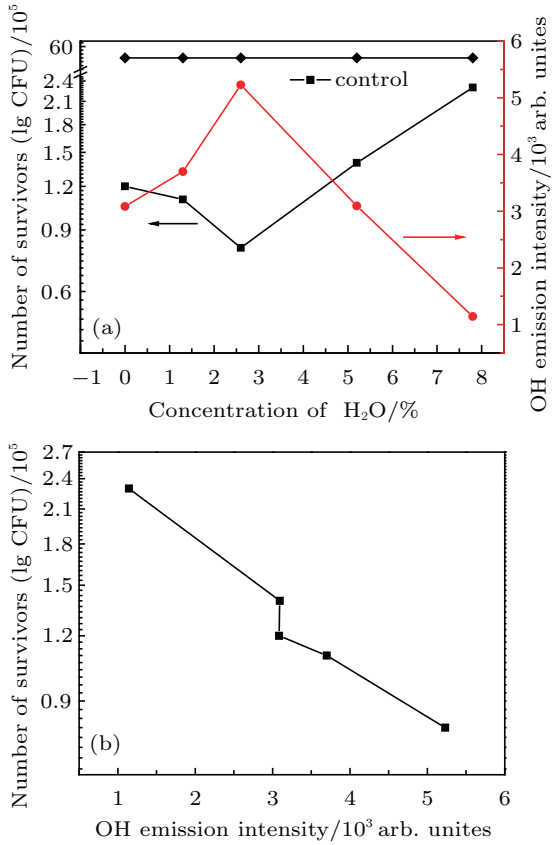


**Fig. 11.** (color online) (a) Survival curves of *Bacillus subtilis* spores and OH intensity as a function of $H_2O$ vapor concentrations (treatment time = 5 min). (b) Survival curves of *Bacillus subtilis* spores as a function of the OH emission intensity (treatment time = 5 min).

To investigate the relationship between the inactivation effects and OH in the Ar and Ar/$H_2O$ plasma jets, the inactivation efficacy as a function of $H_2O$ concentration is determined by counting the surviving spores and the results are compared to the emission of OH. Figure 11(a) shows the killed *Bacillus subtilis* spores as well as actinometric measurements using OH (309 nm) in the Ar/$H_2O$ plasma jet when the $H_2O$ concentration is increased from 0 to 7.8%. The input voltage is 22 kV (peak–peak) and the optimal inactivation efficacy at a specified input voltage is determined by the $H_2O$ concentration. It increases to an optimal value at a specified $H_2O$ vapor concentration and then decreases as the $H_2O$ concentration is increased. The OH emission line intensity also has a maximum value at the specified $H_2O$ concentration. The $H_2O$ vapor concentration corresponding to the optimal inactivation efficacy and maximum OH emission intensity is 2.6 vol% as shown in Fig. 11(a). The number of colony forming units is plotted as a function of the OH emission intensity in Fig. 11(b). It is clear that the inactivation efficacy of spores increases with the OH emission intensity. Compared with the Ar plasma jet, the intensity of the OH emission line increases by 70% at 2.6 vol% $H_2O$, but the inactivation efficiency only increases by 50%. Hence, OH only makes a limited contribution to spore inactivation.

The OH emission line intensity corresponding to 5 vol% $H_2O$ is almost equal to that corresponding to the pure plasma jet, but the inactivation efficacy of the former is worse than that of the latter. OH not only plays a role in spore inactivation, but also alters the charged particles in the Ar or Ar/$H_2O$ plasma jet. Our previous study indicates that spore damage caused by charged particles is the main factor in a pure Ar plasma jet.[36] Hence, a larger electron density will inactivate more spores. According to our results, the electron density of the pure Ar plasma jet is larger than that of the Ar/$H_2O$ plasma jet. As a result, the argon plasma has a higher density and higher inactivation efficacy.

The morphological changes on the *Bacillus subtilis* spores before and after the Ar and Ar/$H_2O$ plasma treatments are shown in the scanning electron microscopy (SEM) images in Fig. 12. The spore images in Figs. 12(a)–12(c) are acquired from the control sample, the sample treated by the Ar plasma jet for 5 min, and the specimen treated by the Ar/$H_2O$ (2.6 vol%) plasma jet for 5 min, respectively. The *Bacillus subtilis* spores exposed to the Ar and Ar/$H_2O$ plasma jets do not exhibit obvious morphological changes. Hence, the charged particles and OH do not produce significant differences in the morphology and our previous results in fact show that the change in the spore shape is primarily due to reactive oxygen species.[36]

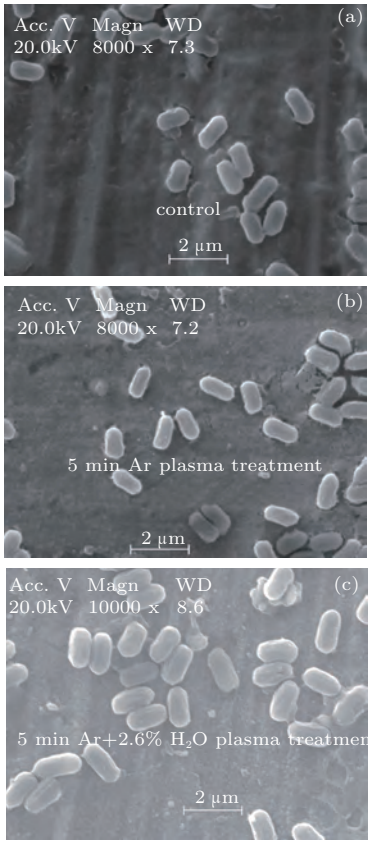


**Fig. 12.** SEM images of *Bacillus subtilis* spores before and after plasma exposure from the control sample (a), sample treated by the Ar plasma jet for 5 min (b), and sample treated by the Ar/$H_2O$ (2.6 vol%) plasma jet for 5 min (c), respectively.

## 4. Conclusion

An atmospheric pressure plasma jet generated with an Ar/$H_2O$ mixture is characterized and the inactivation effects on *Bacillus subtilis* spores are studied. The gas temperature is derived from the rotational temperature of the OH and measured by a thermometer to be about 40 °C. The argon excitation temperature of the pure Ar discharge is estimated to be 0.78 eV. The electron density estimated from Stark broadening of the $H_\beta$ line is on the order of $3.9 \times 10^{14}$ cm$^{-3}$. The gas temperature, excitation electron temperature, and electron density of the plasma jet decrease with increasing water concentration at a fixed input voltage. *Bacillus subtilis* spores are inactivated by the AC atmospheric pressure plasma jet with $H_2O$ in the feedstock gas. The optimal inactivation efficacy is achieved using the appropriate ratio of $H_2O$ to carrier gas. The Ar/$H_2O$ plasma jet results in a more than 0.4-log reduction in the number of spores than that of Ar. Our results reveal that the OH generated by the plasma jet makes a limited contribution to spore inactivation and the spore morphology hardly changes after plasma exposure.

## References


[1] Cheng C, Zhang L Y and Zhan R 2006 *Surf. Coat. Technol.* **200** 6659
[2] Walsh J L and Kong M G 2008 *Appl. Phys. Lett.* **93** 111501
[3] Schäfer J, Foest R, Quade A, Ohl A and Weltmann K D 2008 *J. Phys. D: Appl. Phys.* **41** 194010
[4] Weltmann K, Kindel E, Brandenburg R, Meyer C, Bussiahn R, Wilke C and Woedtke T 2009 *Contrib. Plasma Phys.* **49** 631
[5] Huang C, Yu Q, Hsieh F and Duan Y 2007 *Plasma Proces. Polym.* **4** 77
[6] Cheng C, Liu P, Xu L, Zhang LY, Zhan R J and Zhang W R 2006 *Chin. Phys.* **15** 1544
[7] Uhm H S, Lim J P and Li S Z 2007 *Appl. Phys. Lett.* **90** 261501
[8] Lim J P, Uhm H S and Li S Z 2007 *Phys. Plasmas* **14** 093504
[9] Arnoult G, Cardoso R P, Belmonte T and Henrion G 2008 *Appl. Phys. Lett.* **93** 191507.
[10] Shashurin A, Keidar M, Bronnikov S, Jurjus R A and Stepp M A 2008 *Appl. Phys. Lett.* **93** 181501
[11] Qian M, Ren C, Wang D, Zhang J and Wei G 2010 *J. Appl. Phys.* **107** 063303
[12] Ayan H, Yildirim E D, Pappas D D and Sun W 2011 *Appl. Phys. Lett.* **99** 111502
[13] Cao Z, Walsh J L and Kong M G 2009 *Appl. Phys. Lett.* **94** 021501
[14] Li Q, Li J, Zhu W, Zhu X and Pu Y 2009 *Appl. Phys. Lett.* **95** 141502
[15] Sarani A, Nikiforov A Y and Leys C 2010 *Phys. Plasmas* **17** 063504
[16] Nikiforov A Y, Sarani A and Leys C 2011 *Plasma Sources Sci. Technol.* **20** 015014
[17] Kang S K, Choi M Y, Koo I G, Kim P Y, Kim Y, Kim G J, Mohamed A H, Collins G J and Lee J K 2011 *Appl. Phys. Lett.* **98** 143702
[18] Deng S Xi, Cheng C, Ni G H, Meng Y D and Chen H 2010 *Chin. Phys. B* **19** 105203
[19] Deng S X, Cheng C, Ni G H, Meng Y D and Chen H 2010 *Curr. Appl. Phys.* **10** 1164
[20] Srivastava N and Wang C 2011 *IEEE Trans. Plasma Sci.* **39** 918
[21] Srivastava N and Wang C 2011 *J. Appl. Phys.* **110** 053304
[22] Wang C and Srivastava N 2010 *Eur. Phys. J. D* **60** 465
[23] Kim K, Choi J D, Hong Y C, Kim G, Noh E J, Lee J and Yang S S 2011 *Appl. Phys. Lett.* **98** 073701
[24] Kim S J, Chung T H, Bae S H and Leem S H 2009 *Appl. Phys. Lett.* **94** 141502
[25] Xiong Z, Lu X, Xian Y, Jiang Z and Pan Y 2010 *J. Appl. Phys.* **108** 103303
[26] O'Connora N and Daniels S J 2011 *Appl. Phys.* **110** 013308
[27] Walsh J L and Kong M G 2011 *Appl. Phys. Lett.* **99** 081501
[28] Liu J J and Kong M G 2011 *J. Phys. D: Appl. Phys.* **44** 345203
[29] Sun P, Sun Y, Wu H, Zhu W, Lopez J L, Liu W, Zhang J, Li R and Fang J 2011 *Appl. Phys. Lett.* **98** 021501
[30] Kolb J F, Mohamed A H, Price R O, Swanson R J, Bowman A, Chiavarini R L, Stacey M and Schoenbach K H 2008 *Appl. Phys. Lett.* **92** 241501
[31] Xiong Q, Lu X P, Ostrikov K, Xian Y, Zou C, Xiong Z and Pan Y 2010 *Phys. Plasmas* **17** 043506
[32] Laroussi M 2009 *IEEE Trans. Plasma Sci.* **37** 714
[33] Nagatsu M, Terashita F, Nonaka H, Xu L, Nagata T and Koide Y 2005 *Appl. Phys. Lett.* **86** 211502
[34] Zhao Y, Ogino A and Nagatsua M 2011 *Appl. Phys. Lett.* **98** 191501
[35] Perni S, Shama G, Hobman J L, Lund P A, Kershaw C J, Hidalgo-Arroyo G A, Penn C W, Deng X T, Walsh J L and Kong M G 2007 *Appl. Phys. Lett.* **90** 073902
[36] Shen J, Cheng C, Fang S, Xie H, Lan Y, Ni G, Meng Y, Luo J and Wang X 2012 *Appl. Phys. Express* **5** 036201
[37] Zhu X M, Chen W C and Pu Y K 2008 *J. Phys. D: Appl. Phys.* **41** 105212
[38] Bruggeman P, Verreycken T, Gonzalez M, Walsh J L, Kong M G, Leys C and Schram D C 2010 *J. Phys. D: Appl. Phys.* **43** 124005
[39] Zhang J, Bian X, Chen Q, Liu F and Liu Z 2009 *Chin. Phys. Lett.* **26** 035203
[40] Sáinz A and García M C 2008 *Spectrochim. Acta Part B* **63** 948
[41] Torres J, Jonkers J, van de Sanden M J, van der Mullen J J A M, Gamero A and Sola A 2003 *J. Phys. D: Appl. Phys.* **36** L55
[42] Balcon N, Aanesland A and Boswell R 2007 *Plasma Sources Sci. Technol.* **16** 217
[43] Torres J, van de Sande M J, van der Mullen J J A M, Gamero A and Sola A 2006 *Spectrochim. Acta Part B* **61** 58
[44] Torres J, Palomares J M, Sola A, van der Mullen J J A M and Gamero A 2007 *J. Phys. D: Appl. Phys.* **40** 5929
[45] Konjevic R and Konjevic N 1997 *Spectrochim. Acta Part B* **52** 2077